

11-35  
067143

NASA Technical Memorandum 113124

# Vibrational Analysis of Engine Components Using Neural-Net Processing and Electronic Holography

Arthur J. Decker, E. Brian Fite,  
Oral Mehmed and Scott A. Thorp  
*Lewis Research Center  
Cleveland, Ohio*

Prepared for the  
90th Symposium  
cosponsored by the Advisory Group for Aerospace Research  
and Development and the Propulsion and Energetics Panel  
Brussels, Belgium, October 20–24, 1997



National Aeronautics and  
Space Administration

Trade names or manufacturers' names are used in this report for identification only. This usage does not constitute an official endorsement, either expressed or implied, by the National Aeronautics and Space Administration.

# Vibrational Analysis of Engine Components Using Neural-Net Processing and Electronic Holography

Arthur J. Decker, E. Brian Fite, Oral Mehmed and Scott A. Thorp  
National Aeronautics and Space Administration  
Lewis Research Center  
Cleveland, Ohio 44135  
United States

## 1. SUMMARY

The use of computational-model trained artificial neural networks to acquire damage specific information from electronic holograms is discussed. A neural network is trained to transform two time-average holograms into a pattern related to the bending-induced-strain distribution of the vibrating component. The bending distribution is very sensitive to component damage unlike the characteristic fringe pattern or the displacement amplitude distribution. The neural network processor is fast for real-time visualization of damage. The two-hologram limit makes the processor more robust to speckle pattern decorrelation. Undamaged and cracked cantilever plates serve as effective objects for testing the combination of electronic holography and neural-net processing. The requirements are discussed for using finite-element-model trained neural networks for field inspections of engine components. The paper specifically discusses neural-network fringe pattern analysis in the presence of the laser speckle effect and the performances of two limiting cases of the neural-net architecture.

## 2. INTRODUCTION

As NASA's Turbomachinery Center of Excellence, Lewis Research Center (LeRC) is involved in the testing of various types of rotating machinery including compressors, turbines, fan blades and propellers. Blades are tested in an electronic holography laboratory to obtain frequency and mode shape information for use in wind tunnel and test cell research programs. Over time, this process has been found to be a reliable way of predicting frequencies and mode shapes of blades as well as other test articles. Laboratory electronic holography has become an integral part of the turbomachinery testing, design and fabrication process.

One way to reduce the cost of wind tunnel testing is to inspect components in situ rather than the laboratory. Non-interference inspection to detect crack damage in blades is needed after high vibration stress amplitudes and cycles occur during testing with rotating blades. High stress amplitudes and cycles have been encountered at resonance, flutter and stall conditions during mapping and operability testing of turbojet engine fan models at LeRC. A blade inspection is wise when the stresses exceed the safe stress limits that have been preset.

Removing the blades from a rotor for laboratory inspection for damage or changed vibration characteristics is expensive in terms of lost test time and facilities costs. Hence, whole-field, real-time, in-situ optical inspections using electronic holography are especially attractive. Electronic holography is non-intrusive and has the potential to reduce the number of expensive-to-install, intrusive strain gages needed for wind tunnel testing and for detection of damaged regions.

One defect of electronic holography is that the display of the displacement distribution of a vibrating component may require as many as twelve previously acquired frames.<sup>1</sup> A pipeline processor maintains the illusion of a real-time display, but the speckle patterns must remain correlated between members of sets of twelve frames. That requirement

is hard to maintain outside a laboratory. Regardless, neither the characteristic fringe patterns of classical time-average holography nor the displacement distributions that can be calculated from electronic time-average holography are ideal for inspecting for damage. Instead, the bending induced strain distribution<sup>2</sup> has been shown to be a much better indicator of damage to composites as well as cracking in metals.<sup>3</sup> But the bending distribution must be calculated from a very accurately known displacement distribution.

Artificial neural networks are being tested as alternative processors for electronic holography at LeRC. The goal is to extract damage specific information from as few frames as possible so that electronic holography will be convenient to use for structural inspections in the 9X15 wind tunnel and spin rigs at LeRC. In fact, an electronic hologram can be recorded during a single, electronically shuttered field of a television frame using a continuous wave laser. Short-exposure, time-average holograms can be recorded electronically to achieve the goals suggested for flashlamp pumped dye lasers at another AGARD conference more than ten years earlier.<sup>4</sup> That paper proposed using time-average holography for measuring velocity field information in a flow rather than for measuring structural displacement and strain fields.

The neural network processor requires a computational-model generated training set. The model consists of a phenomenological model and a model of the optical measurement process. A finite element model is the phenomenological model used to compute the predicted vibration modes of a fan blade.<sup>5</sup> A crack model is incorporated for predicting damage. The electronic holography process must be modeled realistically to include a fluctuating laser speckle effect, variations in the sensitivity vector, variations in the CCD camera response and variations in vibration amplitude.<sup>6</sup> A training set consists of records, and a record contains input and output patterns. The input pattern is the characteristic fringe pattern generated by the electronic holography process. The output pattern is a distribution of a component of the bending induced strain.

The trained neural network is then tested for robustness by presenting it with model generated test patterns that vary these factors. Then the neural network is tested with patterns recorded from real structures. The final stage is to encode, compile and link the neural network with the electronic holography video.

The next section discusses the setups, computers and facilities where the work is being done.

## 3. FACILITIES AND EXPERIMENTAL EQUIPMENT

Graphics workstations containing various hardware and software video and graphics options<sup>7</sup> perform the electronic holography and the neural-net processing. The neural networks are generated and trained using a commercial software package.<sup>8</sup> The trained nets are then converted to C language code for linking with the electronic holography software. The performances of the workstation resident

neural networks and electronic holography are discussed later.

Trained neural networks are tested with both model generated and experimental data. The experiments are performed in a holographic vibration analysis laboratory with a large vibration isolation table; argon-ion, helium-neon, diode and Nd:YAG lasers; and several means for mounting and vibrating turbomachinery blades and other components. The laboratory is used routinely for electronic holographic surveys of turbomachinery components and has been used for holography in general since 1976. Lewis Research Center's Low Noise Fan Program and outside industries<sup>9</sup> have been frequent, recent customers.

Electronic holograms are transferred directly to the workstations using ordinary NTSC (American television standard) 30 frame-per-second, 60 field-per-second, CCD (charge coupled device) cameras. The workstations handle as easily PAL (the European television standard). The hardware employs DMA (direct memory access) to transfer the television frames to RAM (random access memory). The workstations are intended specifically to implement color graphics such as OpenGL<sup>10</sup> on color monitors. Hence pixels are packed in multiple byte format. The work reported in this paper used RGBA format consisting of red, green, blue and alpha bytes or RGB\_332\_P format where three colors are packed into a single byte. These formats are really very inefficient for electronic holography which depends on single-byte luminance values.

Processing the holograms in RAM prior to displaying the results can slow down the response considerably. However, we can process a few hundred to a few thousand large pixels (finite element resolutions) while maintaining the 30 frame-per-second display.

A more serious potential problem is frame-to-frame or field-to-field extraneous motions and speckle-pattern decorrelations, particularly outside the laboratory. The actual hologram exposure time can be controlled by the electronic shutters in the CCD cameras. For electronic time-average holography, the shutter needs to be open only for about one vibration cycle. The time between frames can be similarly short, if a locally available high-speed array of CCD cameras is used. Then, bursts of 50,000 or more frames per second become feasible.

LeRC's 9x15-foot wind tunnel is a target facility for applying neural-net processing and electronic holography. Some of the authors have recently been involved with tests of advanced fan models in this wind tunnel. Two of the fan models required blade inspections for crack damage after vibration stresses exceeded preset limits.

Accurate and complete models are critical for effective use of neural-net processing in electronic holography as discussed in the next section.

#### 4. STRUCTURAL AND ELECTRONIC-HOLOGRAPHY MODELS FOR TRAINING ARTIFICIAL NEURAL NETWORKS

The models contain phenomenological and optical components and must generate representative sets of training records. The neural networks must also be trained, by example, to ignore irrelevant variations. For example, the neural networks might be trained to ignore irrelevant variations in mode shapes caused by blade mounting variations. The neural networks must be trained to perform accurately in the presence of the laser speckle effect. Modeling introduces a multidisciplinary expert requirement for using neural networks in electronic holography.

A finite element model is the phenomenological component for this discussion. Finite element models can be used to generate about the first six vibration modes of a blade with good engineering accuracy. A simple cantilever plate serves as the object for this discussion.

Three analytical flat plate models were developed and used as training sets for the neural network. The models simulated both damaged and undamaged plates. All three flat plate models are 7.62 cm (3") wide by 15.24 cm (6") long and have a thickness of 0.254 cm (0.1"). A finite element model was generated consisting of a 20x42 mesh of quadrilateral elements along the mid-thickness of the plate (Figure 1). The plate models were idealized as cantilevered plates with the bottom edge constrained in all six degrees of freedom. The material is 6061-T6 Aluminum with a Young's Modulus of 66.19 GPa ( $9.6 \times 10^6$  psi), a Poisson's Ratio of .33, and a Mass Density of 2712.832 kg/m<sup>3</sup> ( $2.536 \times 10^{-4}$  lbs sec<sup>2</sup>/in<sup>4</sup>).

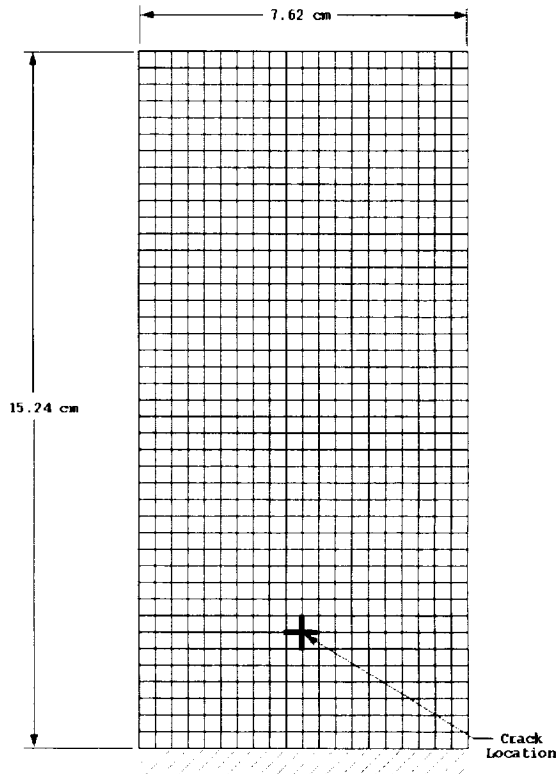


Fig. 1-Finite Element Model.

The first model is a flat plate with no damage included. The second and third models include a vertical and horizontal crack, respectively. Both cracks are located 3.81 cm (1.5") from the long edge and 2.54 cm (1") from the bottom edge. The crack was simulated by creating two coincident grids at this location. The connectivity for the adjacent elements surrounding this location was defined to generate an idealized horizontal crack for the second model ( Fig. 2 ) and a vertical crack for the third model ( Fig. 3 ).

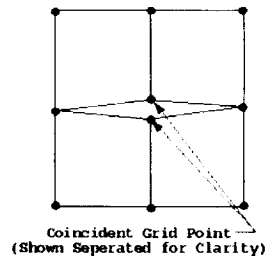
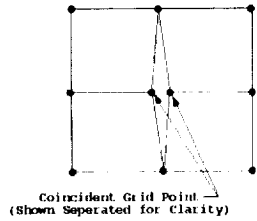


Fig. 2-Horizontal Crack.



**Fig. 3-Vertical Crack.**

MSC/NASTRAN Solution 103 was used to solve for eight normal modes and frequencies. The eigenvectors were normalized with respect to the generalized mass. An output file of the eigenvalues, eigenvectors, and modal strains was then provided to train the neural network.

The optical model of electronic holography in the presence of the laser speckle effect has been discussed in another publication.<sup>6</sup> A training record contains input and output vectors to be received and generated, respectively, by a feed forward artificial neural network. The input vectors contain finite element resolution characteristic fringe patterns. Figure 4<sup>6</sup> shows characteristic fringe patterns, respectively, from an old silver-halide-emulsion time-average hologram of a vibrating blade, from two electronic holograms of a vibrating cantilever plate, from model-generated, finite-element-resolution holograms of a vibrating cantilever plate, and from two finite-element-resolution, electronic holograms of an actual vibrating cantilever plate. The mode shown is the first chord-wise mode of interest in tip cracking of blades. The model generated and measured characteristic fringe patterns appear very similar.

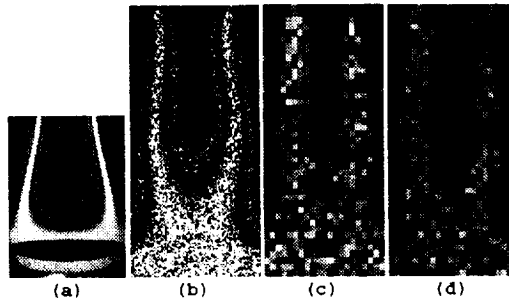


**Fig. 4-First Chord-Wise Mode: (a) Silver Halide Hologram, (b) Electronic Holograms, (c) Model Generated Holograms at Finite Element Resolution, (d) Electronic Holograms at Finite Element Resolution.**

Electronic holography has been discussed in various forms by many authors. Electronic time-average holography is explained very well, for example, by Stetson and Brohinsky.<sup>4</sup> The holographer records image plane holograms consisting of the interferences between smooth reference beams and speckled object beams from vibrating structures. The vibration amplitude distribution can be estimated from twelve holograms containing combinations of hologram-to-hologram phase shifting and phase modulation, if the speckle patterns remain correlated between holograms. The simplest application of electronic time-average holography is accomplished with two frames, where the reference-beam phase is shifted by  $\pi$  between two frames and the frames are subtracted. These actions provide visualization of the characteristic fringe patterns as shown in fig. 4.

The two-frame (or two-field) method of electronic time-average holography supplies the input records for training neural networks. The input patterns are given mathematically by

$$(\text{Speckle Pattern}) \times J_0(2\pi\mathbf{K}\cdot\delta)$$

where  $\delta$  is the displacement vector in wavelengths provided by the finite element modeler and  $\mathbf{K}$  is the sensitivity vector given as the difference between the input and reflected light-ray directions. Speckle patterns in general are modeled with a negative exponential intensity distribution and a uniform phase distribution. The workstations have pseudo random number generators with enormous periods to assure sample-to-sample independence of the speckle patterns. The input patterns are generated from the absolute value of the zero order Bessel function  $J_0$  and are usually normalized between 0 and 1. A saturation effect is sometimes introduced by multiplying the patterns by an arbitrary factor followed by setting inputs greater than 1 at 1.

The model generated output vectors of the training records could contain the displacement amplitude distribution, but a quantity proportional to the bending induced strain is more useful for inspection. Bending induced strain, computed from fringe patterns reconstructed from double-exposure holograms, has been shown to be very sensitive to damage such as cracking.<sup>3</sup> Performing inspection for damage is the principal reason for using neural networks for processing electronic holograms. In fact, visual inspection of characteristic fringe patterns is not a very sensitive way to look for damage. Figure 5 shows characteristic fringe patterns computed from the structural model of a damaged cantilever plate. The damage induced variation in displacement changes by an order of magnitude from picture to picture. Not until the final picture does the characteristic pattern show a significant visual change. Artificial neural networks can be trained to recognize damage much earlier.

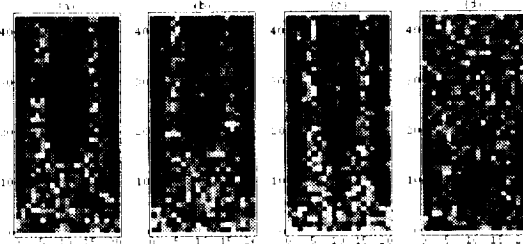


**Fig. 5-Characteristic Patterns for Crack Induced Displacement Changes of (a) 1X, (b) 10X, (c) 100X (d) 1000X the model value.**

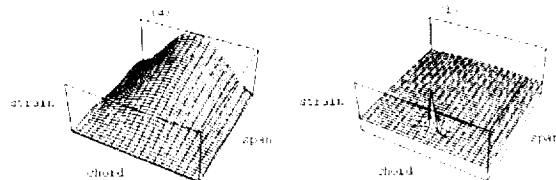


**Fig. 6-Strain Patterns for (a) Undamaged and (b) Cracked Cantilever Plates.**

Surface bending induced strain is computed from the second derivatives of the normal component of displacement.<sup>2</sup> Holography visualizes the quantity  $\mathbf{K}\cdot\delta$ , but  $\mathbf{K}$  often varies slowly enough that the second derivatives of  $\delta$  are adequate.

Figure 6 shows model generated, chord-wise bending induced strain patterns for the mode shown in fig. 4. The patterns are shown for undamaged and cracked samples. The vertical crack model (Fig. 3) was used to generate the patterns.

The formats, training, testing and performances of the neural nets are discussed next.

## 5. NEURAL NETWORKS FOR DETECTING DAMAGED VIBRATING STRUCTURES

This work is based exclusively on feed forward neural networks with one hidden layer. These networks have been divided into two classes: sparse and dense. Sparse neural networks, where the number of hidden-layer nodes is less than 10 percent of the number of inputs, have been discussed for vibrational analysis in another publication.<sup>6</sup> Sparse neural networks train rapidly and can be linked to a workstation's video without degrading the real-time performance. The number of hidden-layer nodes, by contrast, in a dense neural network approaches the number of input nodes or nodes in the finite element model. The parallelized code (loop free) for these networks requires large resources for compilation and linking with the workstation video. The dense nets train slowly and degrade the real-time performance of the workstation video. But the dense nets are more immune to variations in vibration amplitude. The sparse nets yield false readings outside a narrow range of vibration amplitudes. Regardless, the neural networks must be trained to be immune to the laser speckle effect.

The remaining discussion in this section refers to a cantilever plate with the displacement given at 903 nodes. The chord by span arrangement of the nodes is 21 X 43. Blade designs typically use between a few hundred and a few thousand finite elements. The speckle pattern problem can be placed in perspective by noting that there are  $256^{903}$  possible input patterns given an 8-bit dynamic range for representing luminance. But there are only 903 linearly independent patterns. Response surface methods used in the study of sparse nets for vibrational analysis showed that very few hidden-layer nodes and about 10 percent of a set of linearly independent speckle patterns confer immunity to the speckle effect. Only 100 speckle patterns and 6 hidden-layer nodes were needed to train a speckle-effect-immune net to recognize the difference between damaged and undamaged cantilevers. The bending induced strain distributions for this test are shown in fig. 6. Samples of the performance of the neural-net video are discussed in the next section.

The conditions under which the sparse nets can be used to inspect for blade damage are restricted. The nets were able to learn to distinguish only two or three distinct characteristic patterns (different vibration amplitudes) in the amplitude range from 0.25 waves to 0.75 waves of maximum displacement. The sparse nets were actually unable to learn the minimum crack contained in the original models. In fact, successful training required that the effect of the crack be amplified. The modeled damaged and undamaged distributions were subtracted; the difference was multiplied by a factor; and the amplified difference was added to the undamaged amplitude distribution. Figure 5 shows the effect of this process on the calculated characteristic fringe pattern for factors ranging from 1 to 1000. The minimum factor for successful training was 7. The sparse nets still responded with a false identification rate of 20 percent at an amplification factor of 10 (Fig. 5b). The false identification rate was 0 percent for an amplification factor of 100 (Fig. 5c). A more difficult restriction on the use of sparse nets has been the need to control the vibration amplitude to avoid false readings. A network that was model trained at a maximum vibration amplitude of 0.5 waves responded accurately to a set of test examples only when the test amplitudes were controlled within  $\pm 0.05$  wave of 0.5 waves. A point to be noted is that these inspections were used to detect cracks near the base of the cantilever approximation to a blade. A crack was simulated in a physical cantilever by grinding a groove near the position of the modeled crack. The first chord-wise mode (lyre mode) is most sensitive, in fact, for detecting tip cracks.

The response surface study used to optimize the sparse nets showed that the generalization (interpolation and extrapolation) capability of the neural networks improved slowly as the number of hidden-layer nodes was increased. This improvement was found to continue as the number of hidden-layer nodes exceeded 10 percent of the inputs. Subsequently, neural nets were tested on both model generated and measured characteristic patterns where the number of hidden-layer nodes equaled or exceeded 100. The performances of the nets for training and crack identification depended on the crack amplification factor as in the case of the sparse nets. But the dense nets were able to separate damaged from undamaged samples over a larger range of amplitudes than the sparse nets. Non optimized compilation of the parallelized C language code for the neural nets was limited to nets containing about 100 hidden-layer nodes. The object file for a sparse net is less than a megabyte. The object code for a dense net containing 100 hidden-layer nodes is about 10 megabytes. The memory and swap space required for compilation are orders of magnitude larger. Research continues on the use and performance of dense nets as well as sparse nets.

The real-time performance of the neural networks in the video system is discussed next.

## 6. PERFORMANCE OF WORKSTATION RESIDENT NEURAL NETWORKS FOR DAMAGE INSPECTION

Real-time vibrational analysis and inspection using electronic holography and neural-net processing imply image update rates measured in frames per second. The following results were obtained with holograms and synchronization provided by an off-the-shelf monochrome CCD camera and processed and displayed by one of the workstations.<sup>11</sup>

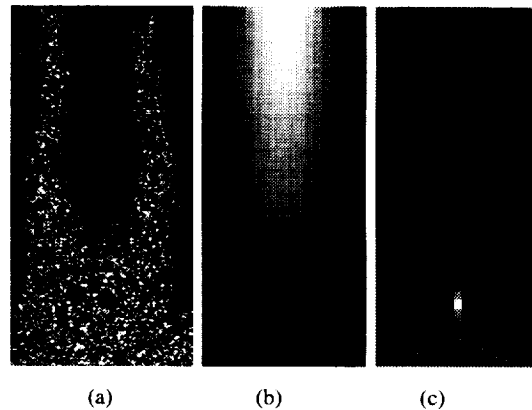


Fig. 7-Video Displays of (a) Characteristic Pattern, (b) Neural-Net Output for Undamaged Cantilever, (c) Neural-Net Output for Cracked Cantilever.

Figure 7 was created from inputs and outputs processed at about  $\frac{1}{2}$  frame per second. Pairs of holograms were captured of cantilevers vibrating in the lyre or first chord-wise mode. A vibrating mirror was synchronized with the CCD camera and was used to shift by  $\pi$  the reference-beam phase between holograms. The 640 X 480 pixel holograms were cropped to the size of the cantilever image (about 153 X 303 pixels); subtracted; zoomed without filtering to the 21 X 43 pixel finite element resolution; converted to binary format; normalized; and processed by the neural network. The output of the neural network was converted to image format, stored, and displayed. Post capture processing was accomplished with the workstation's standard image processing commands and with a slightly modified version of the image subtraction command. This slow processor is very convenient for storing a statistically relevant sample of frames for measuring the false positive and false negative rates for crack detection as

well as measuring the performance of electronic holography in the presence of environmental disturbances. Figure 7a shows a characteristic pattern at about the 153 X 303 pixel resolution; fig. 7b shows a density pattern of the output of the neural network for an uncracked cantilever plate; and fig. 7c shows an output of the neural network for a cracked cantilever plate. The outputs of the neural network are displayed at the 21 X 43 pixel resolution.

The display format at the higher frame rates is the same as shown by fig. 7, but the neural-net and image processing routines must be linked with the workstation's video library. The measured frame rate is about 30 frames per second for the sparse nets containing 6 hidden layer nodes and 903 inputs. The measured frame rate decreases to about 10 frames per second when the number of hidden-layer nodes is increased to 100. Synchronization of the camera, the workstation video, the neural-net processing and the workstation graphics can be challenging at the higher frame rates.

## 7. CONCLUDING REMARKS

Artificial neural networks have been used to process finite-element-resolution time-average fringe patterns at video rates. The full video rates are available to neural networks containing a few hidden-layer nodes. Neural networks with many hidden-layer nodes generalize better, but at slightly lower frame rates. The procedure was developed for electronic holography and vibration analysis, but can be generalized to other applications where there are good phenomenological and visualization models.

The structural application has proven to be very sensitive to small changes in the mode shapes. Perhaps, the major challenge in using the holographic laboratory has been realistic mounting of blades and other components for vibration analysis. The mounting and excitation techniques as well as damage produce subtle variations in the vibration mode shapes. Some of the artificial neural networks are very sensitive to these subtle variations. The work so far has shown that neural networks can be trained to generalize on the laser speckle effect and that dense nets can handle vibration amplitude variations. Whether neural networks can be trained to ignore irrelevant variations in mode shapes remains to be discovered.

To perform a holographic inspection without removing blades from the rotor requires the blades to be seated properly in their retention and vibrated. In model designs at NASA, the blades are normally loose in their retention when the rotor is stationary and are seated during rotation. Thus, a means has to be devised to conveniently seat installed blades to do in-situ damage inspection. This is another challenge that must be overcome to make this method of inspection practical.

As demonstrated in this paper, artificial neural networks can serve as high-speed interfaces between computational models and experiments or tests that generate optical patterns. Whether these interfaces will be efficient, practical and cost effective remains to be discovered.

## 8. REFERENCES

1. K. A. Stetson and W. R. Brohinsky, "Fringe-Shifting Technique for Numerical Analysis of Time-Average Holograms of Vibrating Objects", *J. Opt. Soc. Amer. A5*, pp. 1472-1476, 1988.
2. C. M. Vest, *Holographic Interferometry*, pp. 153-157, Wiley, New York, 1979.
3. A. J. Decker, "Holographic Interferometry with an Injection Seeded Nd:YAG Laser and Two Reference Beams", *Appl. Opt.* **29**, pp. 2696-2700, 1990.
4. A. J. Decker, "Beam-Modulation Methods in Quantitative and Flow-Visualization Holographic Interferometry", *Advanced Instrumentation for Aero Engine Components*, AGARD-CP-399, pp. 34-1 - 34-16, 1986.
5. H. G. Schaeffer, *MSC/NASTRAN Primer Static and Normal Modes Analysis*, PDA Engineering, Costa Mesa, CA, 1979.
6. A. J. Decker, E. Brian Fite, O. Mehmed and Scott A. Thorp, "Processing Speckle Patterns with Model Trained Neural Networks", *Optical Technology in Fluid, Thermal, and Combustion Flow III, Proc. SPIE.* vol. **3172**, to be published.
7. The workstations used to perform the reported research were all vended by Silicon Graphic, Inc., 2011 N. Shoreline Blvd., Mountain View, CA 94043-1389.
8. The neural networks used to perform the reported research were assembled, trained, tested and converted to C language code using *Neural Works Professional II Plus* vended by Neural Ware, Inc., 202 Park West Drive, Pittsburgh, PA 15275.
9. The availability of the holographic vibration analysis laboratory was most recently announced at the *LeRC Business and Industry Summit* held in Sept. 1996.
10. OpenGL Architecture Review Board, *OpenGL Reference Manual*, Addison-Wesley, Reading, MA, 1992.
11. The results were generated with a Silicon Graphics O2 workstation with the R5000 option.

**REPORT DOCUMENTATION PAGE**Form Approved  
OMB No. 0704-0188

Public reporting burden for this collection of information is estimated to average 1 hour per response, including the time for reviewing instructions, searching existing data sources, gathering and maintaining the data needed, and completing and reviewing the collection of information. Send comments regarding this burden estimate or any other aspect of this collection of information, including suggestions for reducing this burden, to Washington Headquarters Services, Directorate for Information Operations and Reports, 1215 Jefferson Davis Highway, Suite 1204, Arlington, VA 22202-4302, and to the Office of Management and Budget, Paperwork Reduction Project (0704-0188), Washington, DC 20503.

<b>1. AGENCY USE ONLY (Leave blank)</b>		<b>2. REPORT DATE</b> September 1997	<b>3. REPORT TYPE AND DATES COVERED</b> Technical Memorandum	
<b>4. TITLE AND SUBTITLE</b> Vibrational Analysis of Engine Components Using Neural-Net Processing and Electronic Holography			<b>5. FUNDING NUMBERS</b>  WU-274-00-00	
<b>6. AUTHOR(S)</b> Arthur J. Decker, E. Brian Fite, Oral Mehmed and Scott A. Thorp				
<b>7. PERFORMING ORGANIZATION NAME(S) AND ADDRESS(ES)</b> National Aeronautics and Space Administration Lewis Research Center Cleveland, Ohio 44135-3191			<b>8. PERFORMING ORGANIZATION REPORT NUMBER</b>  E-10890	
<b>9. SPONSORING/MONITORING AGENCY NAME(S) AND ADDRESS(ES)</b> National Aeronautics and Space Administration Washington, DC 20546-0001			<b>10. SPONSORING/MONITORING AGENCY REPORT NUMBER</b>  NASA TM-113124	
<b>11. SUPPLEMENTARY NOTES</b> Prepared for the 90th Symposium cosponsored by the Advisory Group for Aerospace Research and Development and the Propulsion and Energetics Panel, Brussels, Belgium, October 20-24, 1997. Responsible person, Arthur J. Decker, organization code 5520, (216) 433-3639.				
<b>12a. DISTRIBUTION/AVAILABILITY STATEMENT</b>  Unclassified - Unlimited Subject Category 35  This publication is available from the NASA Center for AeroSpace Information, (301) 621-0390.			<b>12b. DISTRIBUTION CODE</b>	
<b>13. ABSTRACT (Maximum 200 words)</b>  The use of computational-model trained artificial neural networks to acquire damage specific information from electronic holograms is discussed. A neural network is trained to transform two time-average holograms into a pattern related to the bending-induced-strain distribution of the vibrating component. The bending distribution is very sensitive to component damage unlike the characteristic fringe pattern or the displacement amplitude distribution. The neural network processor is fast for real-time visualization of damage. The two-hologram limit makes the processor more robust to speckle pattern decorrelation. Undamaged and cracked cantilever plates serve as effective objects for testing the combination of electronic holography and neural-net processing. The requirements are discussed for using finite-element-model trained neural networks for field inspections of engine components. The paper specifically discusses neural-network fringe pattern analysis in the presence of the laser speckle effect and the performances of two limiting cases of the neural-net architecture.				
<b>14. SUBJECT TERMS</b> Speckle patterns; Neural networks; Electronic holography; Models			<b>15. NUMBER OF PAGES</b> 8	
			<b>16. PRICE CODE</b> A02	
<b>17. SECURITY CLASSIFICATION OF REPORT</b> Unclassified	<b>18. SECURITY CLASSIFICATION OF THIS PAGE</b> Unclassified	<b>19. SECURITY CLASSIFICATION OF ABSTRACT</b> Unclassified	<b>20. LIMITATION OF ABSTRACT</b>	